ORIGINAL ARTICLE Neuro/Head and Neck Radiology

Improving echo-planar imaging-based diffusion weighted imaging of the head and neck using local shim coils

Sven S. Walter[1], Joerg Rothard[2], Mike Notohamiprodjo[1], Miriam Keil[2], Petros Martirosian[1], Sergios Gatidis[1], Konstantin Nikolaou[1]

[1]*Department for Diagnostic and Interventional Radiology, Eberhard Karls University Tuebingen, University Hospital Tuebingen, Germany*

[2]*Siemens Healthcare, Erlangen, Germany*

SUBMISSION: 10/2/2020 - ACCEPTANCE: 25/5/2020

ABSTRACT

Purpose: To evaluate the performance of additional local shim coils within the head/neck surface coil for diffusion-weighted imaging (DWI) MRI of the head/neck region using a 3-Tesla scanner.

Material and Methods: Ten healthy volunteers underwent single-shot echo-planar DWI and T1 gradient echo acquisition of the head/neck region, without (sEPI; sGRE) and with (cEPI; cGRE) the use of additional shim coils integrated into the head/neck coil. Additionally, B_0 field maps with and without additional shim coils were acquired using a dual-echo T1w GRE sequence. Acquisitions were performed on a clinical 3T scanner. In the DWI images, visual evaluation was performed for overall image quality (OAIQ), signal loss, distortions and ghosting. Failure of fat saturation was visually assessed for all sequences. Assessments were quantified using a 4-point scale by two radiologists in consensus. The effects on static field homogeneities were evaluated visually in the acquired field maps. Apparent diffusion coefficients (ADCs) were quantified in the spinal cord, spinal fluid and trapezius muscle for sEPI and cEPI.

Results: Compared to sEPI, cEPI significantly improved OAIQ, distortion and ghosting and decreased signal loss ($p \leq 0.008$). Additionally, cEPI resulted in significantly improved fat saturation compared to sEPI, sGRE and cGRE ($p < 0.001$). Regarding the static magnetic field, additional local shim coils resulted in marked homogenisation, especially in the lower/posterior neck. ADC values did not differ significantly ($p \geq 0.08$).

Conclusions: Additional local shim coils integrated into the head/neck surface coil improve homogenisation of the static magnetic field and providing improved DWI quality compared to standard sEPI. For T1-weighted sGRE, additional coils have no significant effect on fat saturation.

CORRESPONDING AUTHOR, GUARANTOR

Corresponding author: Sven S. Walter, Department for Diagnostic and Interventional Radiology, University Hospital Tuebingen, 3 Hoppe-Seyler-Strasse, 72076 Tuebingen, Germany, Email: sven.walter@med.uni-tuebingen.de

Guarantor: Konstantin Nikolaou, Department for Diagnostic and Interventional Radiology, University Hospital Tuebingen, 3 Hoppe-Seyler-Strasse, 72076 Tuebingen, Germany, Email: Konstantin.Nikolaou@med.uni-tuebingen.de

KEY WORDS
Magnetic resonance imaging; Echo-planar imaging (EPI); Diffusion-weighted imaging (DWI); Head and neck; Shimming; Coils

Introduction

Diffusion-weighted imaging (DWI) is a widely used and increasingly important magnetic resonance imaging (MRI) technique in regular clinical practice. The mechanism of DWI is based on the motion of water molecules through various types of tissue, with more restricted motion in cell-rich tissues such as tumours [1-3]. These diffusion-restricted, cell rich tissues are pictured as areas of hyperintense signal on MRI images [4]. Since the value of DWI was first demonstrated for patients with acute stroke and tumours of the CNS, clinical implementation steadily increased. DWI is now an inherent part of patients suspected ischaemic stroke due to its superiority to non-contrast computed tomography (CT), especially within the first 12 hours after symptom onset [5]. In addition, malignant brain tumours, peritumoural oedema and physiological brain tissue can be differentiated using DWI [6, 7]. DWI is also employed as a means of evaluating for myocardial ischaemia and to detect and stage oncological malignancies and non-oncological diseases, such as inflammatory lesions. In the neck, DWI is specifically used to evaluate for primary tumours and lymph node metastasis in order to measure treatment response and to differentiate between recurring tumours and post-therapeutic changes [3, 8-11]. Furthermore, oriented water diffusivity can be measured by employing diffusion tensor imaging [12].

Of the several DWI techniques used clinically, echo planar imaging (EPI) is employed most commonly due to its rapid acquisition time and resistance to motion-induced phase errors [13, 14]. Several disadvantages of using standard single-shot EPI (sEPI) exist however. These include strong geometric distortions, which occur due to heterogeneous tissues with varying susceptibilities, as well as signal loss and failure of fat saturation due to inhomogeneities of the static magnetic field (B_0) [3, 13, 15-17]. These disadvantages can be further compounded with increasing field strengths [18].

The head and neck region is particularly challenging for echo planar DWI due to air-containing structures and static field inhomogeneities of relative strength with their resulting artefact generation [1, 3]. These inhomogeneities are caused by the complex geometry of this region, as well as strong susceptibility artefacts generated by differences in muscle, adipose, air, blood vessels and their surrounding tissues [2, 9].

Since gradient shimming coils are not able to completely homogenise complex static field inhomogeneities, a potential alternative is the use of additional local shim coils (cEPI). These additional coils are integrated into the lower part of the head and neck surface coil for further improvement of the inhomogeneities of the local static magnetic field, with the goal of improved image quality for EPI based DWI.

The purpose of this study was to evaluate the performance of additional local shim coils within the head and neck surface coil for DWI MRI of the head/neck region using a 3-Tesla machine.

Material and Methods

Study Design

DWI of the head and neck of 10 healthy volunteers (7 males, 3 females, mean age 30.2 ± 4.4 years) were obtained for this study. MR acquisitions were performed on a clinical 3-Tesla scanner (MAGNETOM Vida, Siemens Healthcare, Erlangen, Germany), with the patient in a supine position and the head stabilised with padding on each side of the head/neck surface coil. The head/neck surface coil itself consisted of 20 channels and 2 coil elements. The study was approved by the local ethics committee of the Eberhard Karls University Tuebingen (Germany), and informed consent of all volunteers was obtained.

In all volunteers, a single-shot EPI DWI acquisition of the head/neck region (skull base to shoulders) was performed without (sEPI) and with (cEPI) the use of local shim coils integrated into the lower part of the head/neck coil. In addition, a standard T1-weighted (T1w) gradient echo with spectral fat saturation was performed without (sGRE) and with (cGRE) the use of local shim coils. In order to quantify static field inhomogeneities, B_0 field maps with and without active local

Table 1. Parameters of the acquired sequences with (cEPI, cGRE and cFieldMap) and without (EPI, GRE and FieldMap) additional shim coils.

	Matrix	FoV [mm]	Echo time (TE) [ms]	Repetition time (TR) [ms]	Bandwidth [Hz/pixel]	Slice thickness [mm]	b-values (average) [s/mm²]	Diffusion mode	Fat Saturation mode	Readout segments	Readout partial fourier	Acquisition time [min]
EPI / cEPI	128 x 128	300 x 300	48	13500	2298	5	50 (5) / 800 (12)	3D Diagonal	Standard	35	6/8	4:09
GRE / cGRE	128 x 128	300 x 300	4	49	260	5	-	-	Spectral	35	-	1:19
FieldMap / cFieldMap	128 x 128	300 x 300	12, 46	1000	260	5	-	-	Spectral	35	-	3:18

shim coils were acquired using a dual-echo T1w gradient echo sequence.

Technical Overview

The principal of operation of the local shim feature is the generation of patient-dependent B_0 fields in order to compensate field inhomogeneities induced by the patient. For head and neck applications, field generation is achieved with the help of two independent local shim coil elements. Each local shim coil element consists of multiple windings of copper traces arranged in such a way that the resulting local shim field best aligns to the typical B_0 field inhomogeneities induced by the human body. Corresponding patient-adapted shim currents are required to adjust the individual B_0 field.

For the generation of patient-optimised local shim fields, an accurate knowledge of the disturbed B_0 field is necessary. This is done by a separate sequence, which is measured before the actual clinical sequence. Using this input, the required currents for the local shim coil elements can be calculated.

In order to maximise both adequate image quality and patient safety, special measures were undertaken, which included ensuring decoupling of the local shim coil elements during the transmit phase and decoupling from the gradient system during the transmit and receive phase of the MR acquisition process.

MRI Protocol

The sequence parameters with and without local shim coils are shown in **Table 1**. The same phase encoding direction was used for all EPI sequences.

Visual Analysis

Evaluation was performed in a blinded and randomised fashion by two radiologists in consensus with 7 and 3 years of experience in MRI, respectively. The EPI-based DWI sequences with and without additional local shim coils in the head and neck surface coil were assessed for overall image quality, fat saturation, signal loss, spatial distortions and ghosting. sGRE T1w without and with local shim coils were assessed only for quality of fat saturation. Visual evaluation for all categories was performed on a 4-point Likert scale (1=best possible outcome of the above described category, 4=worst possible outcome).

The effect of local shim coils on the static field distribution was additionally evaluated. To this end, a field map was computed from the dual-echo GRE sequence using vendor-provided software (Syngo Via, Siemens Healthcare, Erlangen, Germany).

Quantitative Analysis

For sEPI and cEPI, the voxel value ± standard deviations of apparent diffusion coefficients (ADC) were measured and compared in three separate anatomical compartments (spinal cord, spinal fluid and trapezius muscle) using circular regions of interest (ROIs).

Statistics

Numerical data are shown as mean ± standard deviation (SD). For comparison of ordinal data, the Friedman test with Bonferroni correction was used, while a T-test was used for continuous data. P-values ≤0.05 were defined as being statistically significant.

Results

Visual analysis

The use of additional local shim coils for single-shot echo planar DWI resulted in a marked improvement

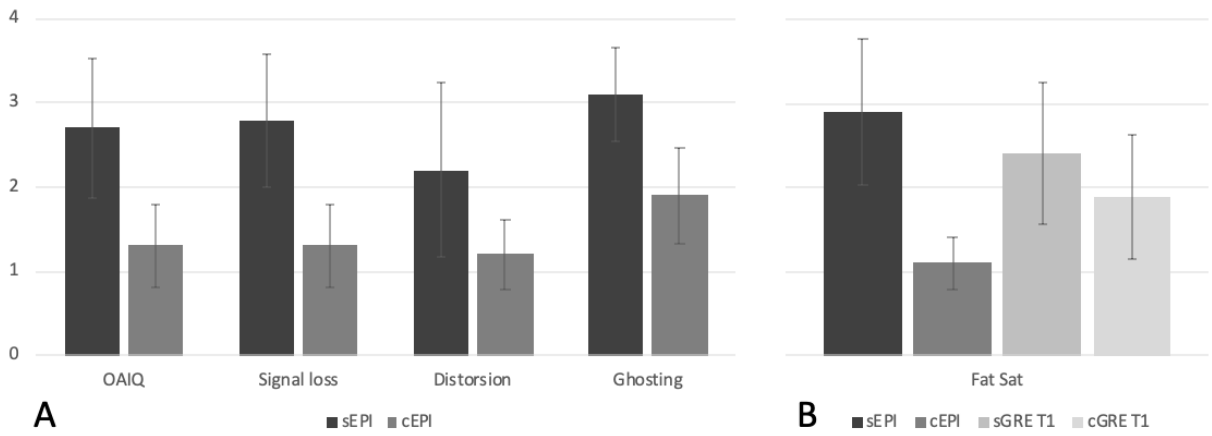

Fig. 1. *Visual image analysis of A: overall image quality (OAIQ), signal loss, distortion, ghosting and B: fat saturation. Data is presented as mean ± standard deviation.*

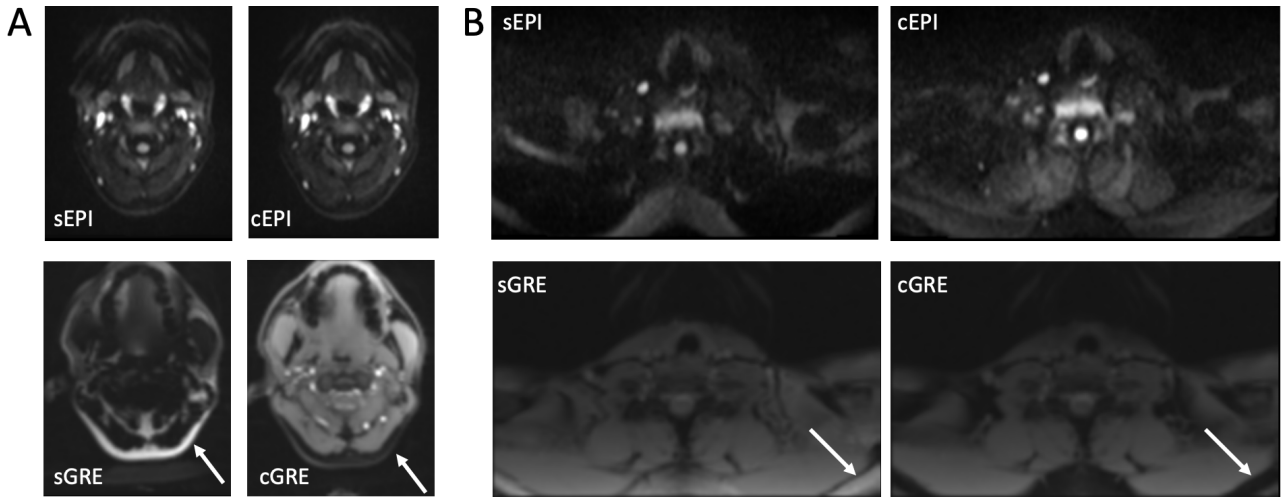

Fig. 2. *Image examples of volunteers. Axial images of the head (A) and shoulder (B) regions with significantly improved image quality, signal loss, distortions and ghosting in cEPI compared to sEPI. Increased fat saturation in cGRE over sGRE, especially in the posterior head and neck regions (arrows).*

of overall image quality compared to EPI without the use of additional coils (p<0.001). Furthermore, signal loss was almost none in cEPI, while sEPI showed significantly increased intermediate levels (p<0.001). The same was seen for distortions between cEPI and sEPI. Although the margin decreased compared to overall image quality and signal loss, spatial distortions were significantly reduced in cEPI (p=0.008). Ghosting artefacts were also significantly reduced in cEPI compared to sEPI (p=0.003) **(Figs. 1, 2)**.

Fat saturation using single-shot EPI without and with the use of additional local shim coils resulted in a significant improvement of cEPI (p<0.001). Furthermore, comparing sGRE and cGRE showed improved fat saturation for cGRE, though not significantly (p=0.177) **(Figs. 1, 2)**.

Comparing the B_0 field maps without and with the use of local shim coils resulted in a marked homogenisation of the static field, especially in the lower and posterior neck regions **(Fig. 3)**.

Quantitative analysis

As described above, the ADC values were quantified in three different anatomical compartments (spinal cord, spinal fluid, trapezius muscles). The measured values did not show significant differences between the acquired sequences for each of the compartments, respectively (p≥0.08; **Fig. 4**).

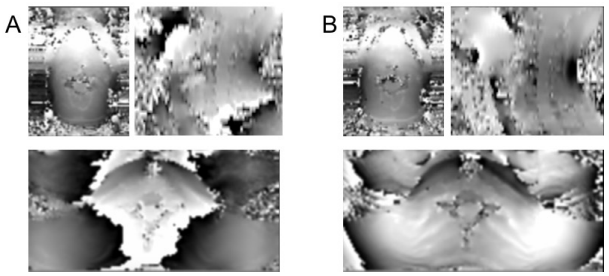

Fig. 3. *B_0 field maps of the head and neck region of sEPI (A) and cEPI (B); (A/B: axial head - top left; sagittal - top right; axial shoulders - bottom).*

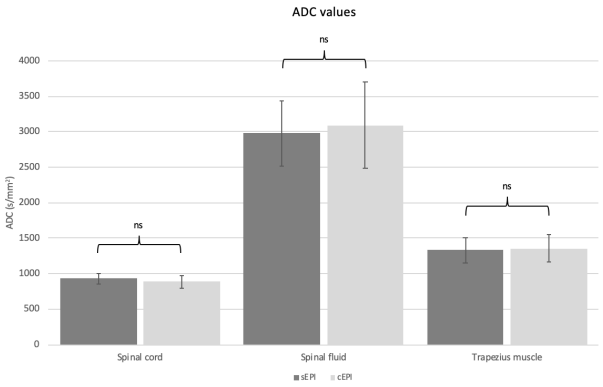

Fig. 4. *ADC quantification within the three anatomical compartments. Data is presented as mm^2/s ± standard deviation; ns: not significant.*

Discussion

In this study, we evaluated a new shimming technique for echo planar DWI and T1w GRE which uses additional local shim coils integrated into the head/neck surface coils at 3-Tesla.

Our results demonstrate that cEPI significantly improves overall image quality, signal loss, distortion and ghosting as compared to sEPI, as well as markedly improves fat saturation compared to sEPI. However, cGRE showed no improvement for the saturation of fat compared to sGRE. Additionally, quantified ADC values showed no significant difference between sEPI and cEPI.

In recent years, several studies have described shimming methods in different regions of the body with significant improvement in resulting images [9, 14, 17, 19-24].

EPI with slice-specific integrated dynamic shimming and frequency adjustment (iEPI) has been shown to improve overall image quality in the head and neck region due to the improved homogenisation of the magnetic field, resulting in a reduction of artefacts [25]. This was also shown in a recent study by Chen et al. (2018) who assessed 21 patients with thyroid nodules for the image quality of integrated shimming compared to 3D volume shimming EPI [23]. However, iEPI cannot be combined with simultaneous-multi-slice (SMS) imaging for the purpose of reducing examination time.

In a study with 74 breast cancer patients, Kim et al. demonstrated superiority in image quality of readout-segmented EPI (rsEPI), which reduces the effect of B_0 field inhomogeneities by shortening the echo spacing as compared to sEPI [9, 26]. In addition, it has been shown by our group that combining the above mentioned iEPI and rsEPI (irsEPI) resulted in a further improvement in MR imaging of the head and neck region [9]. However, comparing cEPI and irsEPI, the currently described method has the additional advantage of reduction in acquisition time, as well as the added ability to use inversion recovery fat saturation (SPAIR).

The results of the quantification of ADC values are similar with previous studies, which demonstrated no significant differences in the measurements. However, it should be noted that most previous studies analysed different anatomical structures and compared different shimming techniques [9, 23, 27]. Yet, the measured anatomical structures in this study were chosen to cover a wide range of ADC-values.

In general, the rapid improvement in MRI of the head and neck region has resulted in improved clinical diagnosis. Consequently, further assessments of different kinds of pathologies in the head and neck region are necessary [28]. Specifically, primary tumours that occur in the oral cavity, pharynx, larynx, salivary glands, thyroid, soft tissue as well as neural structures and lymph node metastasis should be assessed. Furthermore, additional evaluation of treatment response as well as differentiation between recurring tumours and post-therapeutic change is necessary [4, 8, 9, 11, 29]. The results of this study show that additional local shim coils implemented in the head and neck surface coil improve image quality and homogeneity of the magnetic field without altering scan time, leading to potentially improved clinical evaluation of these pathologies.

This study has several limitations. In the clinical setting, patients' compliance may be reduced during MR ex-

aminations as compared to health volunteers, resulting in increased motion artefact. Thus, further evaluation of the clinical significance of our results in DWI are necessary. Although quantitively measurable with distortion ratio, signal-to-noise ratio, and contrast-to-noise ratio, image analysis was only performed on a subjective basis. Furthermore, the described improvement in image quality and increased homogeneity of the magnetic field does not necessarily translate to improvement in clinical diagnostics and resulting therapeutic decisions. In order to explore these limitations, a larger sample size in disease-specific cohorts is required. Lastly, the MR scanner that was used for this study has only the described echo planar DWI shimming sequences (sEPI, cEPI). Thus, we were not able to compare this new shimming technique to clinically proven techniques such as slice-specific integrated dynamic shimming.

In the future, cEPI may be combined with simultaneous-multi-slice to further reduce examination time.

Conclusion

Additional local shim coils integrated into the head/neck surface coil improve homogenisation of the static magnetic field and providing improved DWI quality compared to standard sEPI. For T1w sGRE, additional coils have no significant effect on fat saturation. **R**

Funding

This project did not receive any specific funding.

Ethical approval

The study was approved by the local ethics committee of the Eberhard Karls University Tuebingen (Germany), and informed consent of all volunteers was obtained.

Conflict of interest

Miriam Keil and Joerg Rothard are employees of Siemens Healthcare.

References

1. Bae YJ, Choi BS, Jeong HK, et al. Diffusion-weighted imaging of the head and neck: influence of fat-suppression technique and multishot 2D navigated interleaved acquisitions. *AJNR Am J Neuroradiol* 2018; 39(1): 145-150.
2. Hirata K, Nakaura T, Okuaki T. Comparison of the image quality of turbo spin echo- and echo-planar diffusion-weighted images of the oral cavity. *Medicine (Baltimore)* 2018; 97(19): e0447.
3. Mikayama R, Yabuuchi H, Sonoda S, et al. Comparison of intravoxel incoherent motion diffusion-weighted imaging between turbo spin-echo and echo-planar imaging of the head and neck. *Eur Radiol* 2018; 28(1): 316-324.
4. Chilla GS, Tan CH, Xu C. Diffusion weighted magnetic resonance imaging and its recent trend-a survey. *Quant Imaging Med Surg* 2015; 5(3): 407-422.
5. Schellinger PD, Bryan RN, Caplan LR. Evidence-based guideline: The role of diffusion and perfusion MRI for the diagnosis of acute ischemic stroke: report of the therapeutics and technology assessment subcommittee of the american academy of neurology. *Neurology* 2010; 75(2): 177-185.
6. Fung SH, Roccatagliata L, Gonzalez RG. MR diffusion imaging in ischemic stroke. *Neuroimaging Clin N Am* 2011; 21(2): 345-377, xi.
7. Maier SE, Sun Y, Mulkern RV. Diffusion imaging of brain tumours. *NMR Biomed* 2010; 23(7): 849-864.
8. Ma G, Xu XQ, Hu H, et al. Utility of readout-segmented echo-planar imaging-based diffusion kurtosis imaging for differentiating malignant from benign masses in head and neck region. *Korean J Radiol* 2018; 19(3): 443-451.
9. Walter SS, Liu W, Stemmer A, et al. Combination of integrated dynamic shimming and readout-segmented echo planar imaging for diffusion weighted MRI of the head and neck region at 3Tesla. *Magn Reson Imaging* 2017; 42: 32-36.
10. Jin J, Chen M, Li Y, et al. Detecting acute myocardial infarction by diffusion-weighted versus T2-weighted imaging and myocardial necrosis markers. *Tex Heart Inst J* 2016; 43(5): 383-391.
11. Chawla S, Kim S, Wangl S, et al. Diffusion-weighted imaging in head and neck cancers. *Future Oncol* 2009; 5(7): 959-975.
12. Soares JM, Marques P, Alves V, et al. A hitchhiker's

guide to diffusion tensor imaging. *Front Neurosci* 2013; 7: 31.
13. Yoshida T, Urikura A, Shirata K, et al. Image quality assessment of single-shot turbo spin echo diffusion-weighted imaging with parallel imaging technique: a phantom study. *Br J Radiol* 2016; 89(1065): 20160512.
14. Andre JB, Bammer R. Advanced diffusion-weighted magnetic resonance imaging techniques of the human spinal cord. *Top Magn Reson Imaging* 2010; 21(6): 367-378.
15. Olman CA, Davachi L, Inati S. Distortion and signal loss in medial temporal lobe. *PLoS One* 2009; 4(12): e8160.
16. Thoeny HC, De Keyzer F, King AD. Diffusion-weighted MR Imaging in the Head and Neck. *Radiology* 2012; 263(1): 19-32.
17. Stockmann JP, Wald LL. In vivo B0 field shimming methods for MRI at 7T. *Neuroimage* 2018; 168: 71-87.
18. Lavdas I, Miquel ME, McRobbie DW, et al. Comparison between diffusion-weighted MRI (DW-MRI) at 1.5 and 3 tesla: a phantom study. *J Magn Reson Imaging* 2014; 40(3): 682-690.
19. Porter DA, Heidemann RM. High resolution diffusion-weighted imaging using readout-segmented echo-planar imaging, parallel imaging and a two-dimensional navigator-based reacquisition. *Magn Reson Med* 2009; 62(2): 468-475.
20. Filipe JP, Curvo-Semedo L, Casalta-Lopeset J, et al. Diffusion-weighted imaging of the liver: usefulness of ADC values in the differential diagnosis of focal lesions and effect of ROI methods on ADC measurements. *MAGMA* 2013; 26(3): 303-312.
21. Zhang H, Xue H, Stemmer A, et al. Integrated shimming improves lesion detection in Whole-Body Diffusion-Weighted examinations of patients with plasma disorder at 3 T. *Invest Radiol* 2016; 51(5): 297-305.
22. Barth BK, Cornelius A, Nanzet D, et al. Diffusion-Weighted Imaging of the prostate: Image quality and geometric distortion of Readout-Segmented versus Selective-Excitation Accelerated Acquisitions. *Invest Radiol* 2015; 50(11): 785-791.
23. Chen L, Sun P, Hao Q, et al. Diffusion-weighted MRI in the evaluation of the thyroid nodule: Comparison between integrated-shimming EPI and conventional 3D-shimming EPI techniques. *Oncotarget* 2018; 9(40): 26209-26216.
24. Darnell D, Truong TK, Song AW. Integrated parallel reception, excitation, and shimming (iPRES) with multiple shim loops per radio-frequency coil element for improved B0 shimming. *Magn Reson Med* 2017; 77(5): 2077-2086.
25. Stemmer A, Kiefer B. Combination of integrated slice-specific dynamic shimming and pixel-wise unwarping of residual EPI distortions. *Proc Int Soc Magn Reson Med* 2015; Abstract #3729.
26. Kim YJ, Kim SH, Kang BJ, et al. Readout-segmented echo-planar imaging in diffusion-weighted mr imaging in breast cancer: comparison with single-shot echo-planar imaging in image quality. *Korean J Radiol* 2014; 15(4): 403-410.
27. Li H, Liu L, Shiet Q, et al. Bladder cancer: detection and image quality compared among iShim, RESOLVE, and ss-EPI diffusion-weighted MR imaging with high b value at 3.0 T MRI. *Medicine (Baltimore)* 2017; 96(50): e9292.
28. Gatidis S, Graf H, Weiß J, et al. Diffusion-weighted echo planar MR imaging of the neck at 3 T using integrated shimming: comparison of MR sequence techniques for reducing artifacts caused by magnetic-field inhomogeneities. *MAGMA* 2017; 30(1): 57-63.
29. Heroiu Cataloiu AD, Danciu CE, Popescu CR. Multiple cancers of the head and neck. *Maedica (Buchar)* 2013; 8(1): 80-85.

READY - MADE CITATION

Walter SS, Rothard J, Notohamiprodjo M, Keil M, Martirosian P, Gatidis S, Nikolaou K. Improving echo-planar imaging-based diffusion weighted imaging of the head and neck using local shim coils. *Hell J Radiol 2020*; 5(3): 4-10.